Rapid Communications

Electron affinity of the hafnium atom

Rulin Tang,[1] Xiaolin Chen,[1] Xiaoxi Fu,[1] Huan Wang,[1] and Chuangang Ning[1,2,*]

[1]*Department of Physics, State Key Laboratory of Low-Dimensional Quantum Physics, Tsinghua University, Beijing 10084, China*

[2]*Collaborative Innovation Center of Quantum Matter, Beijing, China*

(Received 31 May 2018; published 6 August 2018)

Hafnium is the last transition-metal element with an undetermined electron affinity. Using a slow-electron velocity-map imaging spectrometer equipped with a cold ion trap, the electron affinity of hafnium atoms is measured to be 1436(5) cm^{-1} or 0.1780(6) eV. The cold ion trap employed in the present measurement is found to be crucial for reducing the background noise from the hafnium hydride anions.

DOI: 10.1103/PhysRevA.98.020501

The electron affinity (EA) measures the capability of an atom to form the corresponding negative ion. It is a fundamental parameter for understanding chemical reactions. Efforts towards the completion of a periodic table for atomic negative ions [1,2] for more than a half century have established that most atomic elements can form stable negative ions and their electron affinities have been accurately measured [3–8]. Hafnium is the last transition-metal element whose electron affinity remains to be determined apart from the radioactive elements. In 1981, Feigerle *et al.* employed a Cs^+ sputter source to produce Hf^- ions, and investigated their electronic structure via laser photoelectron spectroscopy (LPES). The low signal-to-noise ratio [9] prevented them from reaching a definite conclusion regarding the stability of Hf^-. The lack of definitive experimental evidence for its stability persists in the latest review for atomic negative ions by Andersen [4], although Nadeau *et al.* established a lower limit for its EA: $\geqslant$0.1 eV based on accelerator mass spectrometry (AMS) [10]. Recently, a lower limit of EA $\geqslant$ 0 eV was provided by Davis *et al.* based on LPES [11]. A theoretically predicted value of 0.017 eV was presented by Felfli *et al.* via the Regge-pole calculations [12]. Using relativistic configuration interaction calculations [13], Pan and Beck predicted that Hf^- has one bound state $5d^26s^26p\ J = 5/2$ and EA is 0.114 eV. The EA of Hf remains to be measured.

Our group has in recent years significantly improved the accuracies of EA measurements for several transition-metal elements employing the method of slow-electron velocity-map imaging (SEVI) [14–17]. For instance, we reported the high-accuracy EA value of 0.91 740(6) eV for Nb atoms [14]. The details about the SEVI spectrometer were described previously [16]. In brief, the apparatus consists of a laser ablation ion source, a time-of-flight (TOF) mass spectrometer, and a photoelectron velocity-map imaging (VMI) system [18–20]. Efforts to measure the EA of Hf atoms in our SEVI spectrometer started two years ago. The 532-nm light from a pulsed Nd:YAG laser ($\sim$10 mJ/pulse) is focused onto a rotating and translating hafnium metal disk. Ions are produced via the pulsed laser ablation ion source operating at a 20-Hz repetition rate. They are extracted and accelerated by a TOF mass spectrometer. In the process, Hf^- ions are selected by a mass gate, and are photodetached by a tunable dye laser in the interaction region of the velocity-map imaging system. The outgoing photoelectrons are projected onto a phosphor screen enhanced by a set of microchannel plates and recorded by a charge-coupled device (CCD) camera. During the flight from the photodetachment zone to the phosphor screen, the photoelectrons with the same kinetic energy form a spherical shell with the radius r proportional to the velocity. This enables the photoelectron kinetic energy E_k to be determined using the relationship $E_k = \alpha r^2$, where the coefficient α can be determined via an energy calibration. With the polarization vector of the linearly polarized dye laser beam parallel to the screen, the distribution of the projected photoelectrons exhibits a cylindrical symmetry with respect to the polarization. The three-dimensional photoelectron distribution can thus be reconstructed from the projected two-dimensional image. In the work reported here, this reconstruction is carried out by the method of maximum entropy [21].

A typical mass spectrum we obtained via the laser ablation ion source is shown in Fig. 1. The dominant signals are from hafnium hydride anions HfH^- and HfH_2^-. No indications are observed that the hydride negative ion signals would become weaker after a prolonged laser ablation, presumably due to the high reactivity of hafnium with the small-mass hydrogen atoms, which can easily diffuse into the metal lattices. Our experiences show that the hydride anion signals are always dominant in the laser ablation of any early transition metal, consistent with what happened in the Cs^+ sputter sources [22]. Actually, we note that titanium, an element in the same group as hafnium, is used to absorb H_2 gas in a titanium sublimation pump. The natural abundances of the isotopes of hafnium are ^{176}Hf 5.26%, ^{177}Hf 18.60%, ^{178}Hf 27.28%, ^{179}Hf 13.62%, and ^{180}Hf 35.08% . As shown in Fig. 1, the $m = 176$ signal is composed of pure $^{176}Hf^-$, although its quantity is too small for the subsequent photodetachment experiment. Other mass signals all contain significant hydride contaminations from the isotope distribution. Preliminary experiments show that the photoelectron signal from Hf^- is overwhelmed by those from HfH^- and HfH_2^-. During the trial period, we spot a weak line in the photoelectron energy spectra for $m = 177$, very likely

*ningcg@tsinghua.edu.cn

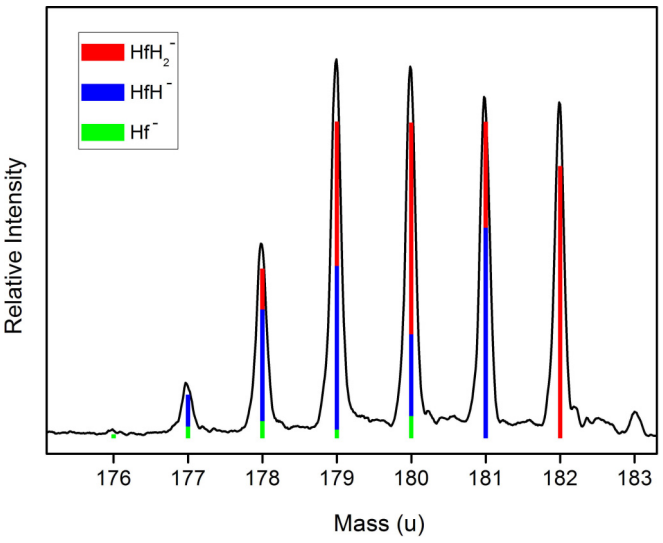

FIG. 1. Mass spectrum of laser ablation on a hafnium metal disk. The vertical color sticks indicate the composition of each peak according to the natural abundance of Hf isotopes. Green bars stand for Hf^- anions, blue for HfH^-, red for HfH_2^-.

to be from Hf^-. However, the signal-to-noise ratio is not good enough for the measurement of the EA. In fact, this weak signal is nearly buried in the noisy background contaminated by hafnium hydride anions. The hydride anions produced via the laser ablation are usually very hot, and hot bands and thermal broadening almost turn the photoelectron energy spectra of hydride anions into a continuum background.

To overcome the above bottleneck, a cold ion trap was built and augmented into our apparatus recently. This octupole radio-frequency (rf) ion trap is mounted on a cryogenic cold head, which is capable of cooling molecular anions down to a temperature as low as ~10 K through collisions with the buffer gas ($He : H_2 = 4 : 1$). The ions are trapped and cooled in the trap for 45 ms. It substantially improves the sharpness and cleanness of the photoelectron energy spectra of molecular anions [23–26]. Moreover, the ion trap can accumulate ions to enhance the ion intensity. Figure 2 shows the photoelectron energy spectra for $m = 177$, 180, 181, and 182 at the photon energy $h\nu = 15\,354\,\mathrm{cm}^{-1}$ with the ion trap operating at a nominal temperature of 15 K. The temperature of trapped ions is usually slightly higher due to rf heating. As shown in Fig. 1, the signals for $m = 177$ include both $^{177}Hf^-$ and $^{176}HfH^-$; those for $m = 180$ include $^{180}Hf^-$, $^{179}HfH^-$, and $^{178}HfH_2^-$; those for $m = 181$ include $^{180}HfH^-$ and $^{179}HfH_2^-$; and those for $m = 182$ are pure $^{180}HfH_2^-$. Peaks a and b appear in the photoelectron energy spectra for $m = 177$ and 180, but disappear for $m = 181$ and 182. Therefore, it is reasonable to conclude that both peaks a and b are from Hf^-.

Based on the calculations by Pan and Beck [13], the dominant signal in the photoelectron spectrum of Hf^- should be the $6p$ detachment into the Hf I ground state $5d^26s^2\,{}^3F_2$. This prediction agrees with the observed spectra in Figs. 2 and 3. Moreover, the velocity-map imaging method can obtain the anisotropic parameter β for the photoelectron angular distribution. The measured β value for peak a is 1.1, and 0.7 for peak b. This is consistent with the expected detachment of a

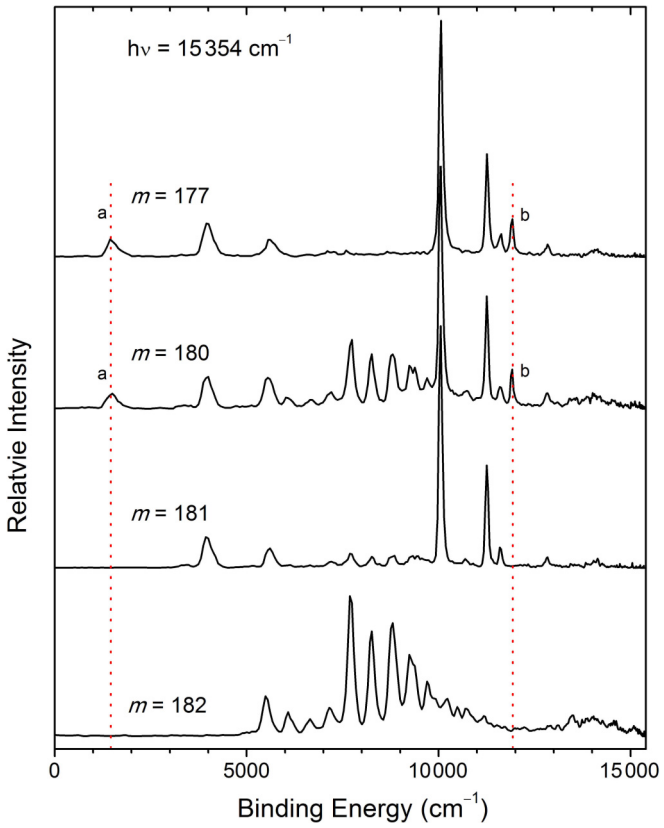

FIG. 2. Photoelectron spectra of anions produced by laser ablation on a hafnium metal disk at the photon energy $h\nu = 15\,354\,\mathrm{cm}^{-1}$. The anions with $m = 177$ include $^{177}Hf^-$ and $^{176}HfH^-$; those with $m = 180$ include $^{180}Hf^-$, $^{179}HfH^-$, $^{177}HfH_2^-$; those with $m = 181$ include $^{180}HfH^-$ and $^{179}HfH_2^-$; and those with $m = 182$ are pure $^{180}HfH_2^-$. The dotted lines indicated that peaks a and b are from atomic anions Hf^-.

p electron. According to the measured binding energies, peak a should be due to the transition from $Hf^-\ 5d^26s^26p\ J = 5/2$ to Hf $5d^26s^2\,{}^3F_2$, and peak b should be due to the transition from $Hf^-5d^26s^26p\ J = 5/2$ to Hf $5d^26s^2\,{}^1G_4$. The binding energy of peak a is unfortunately out of the tuning range of our dye laser for the measurement around the photodetachment threshold. Therefore, the channel related to peak b is chosen for the EA measurement. However, as shown in Fig. 3(a), peak b nearly disappears at $h\nu = 12\,760\,\mathrm{cm}^{-1}$, which is unusual for photodetaching a p electron. The intensity of peak b is observed to decrease much faster than the Wigner threshold law relation $\sigma \propto (E_k)^{1/2}$ as the photon energy decreases [27], with E_k denoting the photoelectron kinetic energy and σ the total photodetachment cross section. To study this in detail, we record the intensity of peak b as a function of the photon energy $h\nu$ from $14\,111\,\mathrm{cm}^{-1}$ to $15\,852\,\mathrm{cm}^{-1}$. To overcome the intensity fluctuation of ion beams, the intensity ratio of peak b to peak a is plotted in Fig. 3(b). It is reasonable to assume that the intensity of peak a does not change much as $h\nu$ changes, because the change to the kinetic energy of peak a is relatively small. As clearly revealed in Fig. 3(b), the transition corresponding to peak b is a broad resonance, centered at $15\,086\,\mathrm{cm}^{-1}$ with a width of $590\,\mathrm{cm}^{-1}$. According to the calculations by Pan and Beck [13], the dominant LS

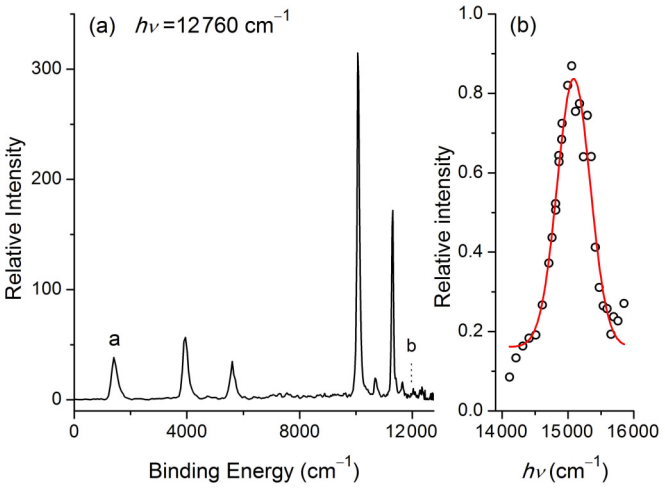

FIG. 3. Photoelectron spectrum of anions with $m = 177$ (^{177}Hf$^-$ and ^{176}HfH$^-$) at the photon energy $h\nu = 12\,760\,\mathrm{cm}^{-1}$ (a); the resonance related to peak b. The open circles are experimental data. The red curve comes from the fitting to a Gaussian function (b).

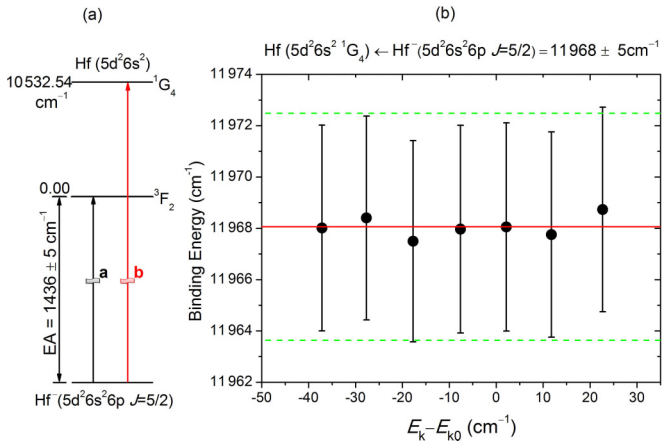

FIG. 4. Transitions related to the present measurement (a); measured binding energy of the transition Hf($5d^26s^2$ $^1G_4$) ← Hf$^-$($5d^26s^26p$ $J = 5/2$) according to Eq. (1). E_k is the kinetic energy of peak b. E_{k0} is the kinetic energy of the calibration transition Re($5d^66s$ $^6D_{9/2}$) ← Re$^-$($5d^66s^2$ $^5D_4$). The photon energy $h\nu$ is tuned to change the difference between E_k and E_{k0}. The dashed lines indicate the $\pm 5\,\mathrm{cm}^{-1}$ uncertainty (b).

terms of the Hf$^-$ ground state $5d^26s^26p$ $J = 5/2$ are $^4G_{5/2}$ (68%) and $^2F_{5/2}$ (27%). The photodetachment channel b has a strong mixing with a large resonance state $5d6s^26p^2\,^2G_{7/2}$ via an electric-dipole transition from the Hf$^-$ ground state ($^2F_{5/2}$ composition). Consequently, the method that we used before for accurately measuring the EA around the photodetachment threshold cannot be used for the EA measurement of Hf. The intensity of peak b is too weak around its detachment threshold.

Since the measured photoelectron kinetic energy usually has a non-negligible deviation from the relation $E_k = \alpha r^2$ in a large dynamic range, a local linear interpolation method based on a known atomic transition is used to determine the binding energies of peaks a and b as accurately as possible; i.e., the following equation

$$E_k = E_{k0} + \alpha(r^2 - r_0{}^2), \tag{1}$$

is used to determine the kinetic energy instead of the simple relation $E_k = \alpha r^2$, where E_k and r are the kinetic energy and radius of the peak to be measured, and E_{k0} and r_0 correspond to the calibration transition. α is still the energy calibration coefficient. If $r \approx r_0$, compared with $E_k = \alpha r^2$, the present interpolation method leads to a smaller error. In the present work, rhenium anions Re$^-$ are used for the energy calibration. The EA of Re atom is 487.13(51) cm^{-1}, close to the EA of Hf [28]. Moreover, Re$^-$ has five sharp lines at the photon energy 15 610 cm^{-1}, which can be used to obtain α. The transition from the ground state $^5D_4$ of Re$^-$ to Re $5d^56s^2\,^6S_{5/2}$ is chosen to determine E_k of peak a. The transition from Re$^-$ $^5D_4$ to Re $5d^66s\,^6D_{9/2}$ is chosen for peak b. The energy level of Re $^6D_{9/2}$ is 11 754.52 cm^{-1} above the ground state $^6S_{5/2}$ of Re [29]. Based on Eq. (1), when probing the calibration transitions, the photon energy is tuned so that the kinetic energy, E_{k0}, is close to that of the target transition, E_k. As shown in Fig. 4, the binding energy of peak b is determined to be 11 968 cm^{-1} with an uncertainty $\pm 5\,\mathrm{cm}^{-1}$. In Eq. (1), $E_{k0} = h\nu_0 - \mathrm{BE}_0$ can be considered as an accurate value because the photon energy $h\nu_0$ is monitored via a wavelength meter with an accuracy 0.02 cm^{-1} and BE$_0$, the binding energies of Re$^-$, are accurately known [28]. The linewidth of our dye laser is 0.06 cm^{-1}. The uncertainty is thus mainly contributed by the measurement errors of the radii, which are obtained by fitting to a Gaussian function. The resulting uncertainty of $\pm 5\,\mathrm{cm}^{-1}$ includes the possible systematic errors, which are estimated in four independent measurements. Similarly, the binding energy of peak a is determined to be $1449 \pm 30\,\mathrm{cm}^{-1}$. The energy difference between peaks a and b obtained in the present measurement is 10 519(30) cm^{-1}, which agrees well with the energy gap 10 532.54 cm^{-1} between the $^1G_4$ and $^3F_2$ states of Hf [29]. This further confirms the assignments that both peaks a and b are from Hf$^-$. The energy level of $^1G_4$ is 10 532.54 cm^{-1} above the ground state $^3F_2$ of Hf. Therefore, after subtracting 10 532.54 cm^{-1} from the binding energy of peak b 11 968(5) cm^{-1}, we determine the electron affinity of Hf to be 1436(5) cm^{-1} or 0.1780(6) eV. This is in reasonable agreement with the previous theoretical EA value 0.114 eV predicted by Pan and Beck [13], considering the complexity of the electronic structures of Hf$^-$ and Hf. The EA value 0.017 eV predicted by Felfli *et al.* has a much larger deviation [12].

In conclusion, we report a measured value of the electron affinity of hafnium atoms to be 1436(5) cm^{-1} or 0.1780(6) eV via the slow-electron velocity-map imaging method. This measurement is made possible by the addition of a cold ion trap, which reduces the background noise from the hafnium hydride anions. The overcoming of hydride contamination commonly faced in measuring the electron affinities of early transition metals and some lanthanides represents a significant breakthrough. This work highlights the power of the combination of the slow-electron velocity-map imaging method and a cold ion trap in accurate measurement of electron affinities.

This work is supported by the National Natural Science Foundation of China (NSFC) (Grants No. 91336104 and No. 91736102).

[1] W. C. Lineberger, Annu. Rev. Phys. Chem. **64**, 21 (2013).
[2] L. M. Branscomb, D. S. Burch, S. J. Smith, and S. Geltman, Phys. Rev. **111**, 504 (1958).
[3] T. Andersen, H. K. Haugen, and H. Hotop, J. Phys. Chem. Ref. Data **28**, 1511 (1999).
[4] T. Andersen, Phys. Rep. **394**, 157 (2004).
[5] C. Blondel, C. Delsart, and F. Dulieu, Phys. Rev. Lett. **77**, 3755 (1996).
[6] M. Scheer, R. C. Bilodeau, and H. K. Haugen, Phys. Rev. Lett. **80**, 2562 (1998).
[7] D. Bresteau, C. Drag, and C. Blondel, Phys. Rev. A **93**, 013414 (2016).
[8] C. W. Walter, N. D. Gibson, D. J. Carman, Y. G. Li, and D. J. Matyas, Phys. Rev. A **82**, 032507 (2010).
[9] C. S. Feigerle, R. R. Corderman, S. V. Bobashev, and W. C. Lineberger, J. Chem. Phys. **74**, 1580 (1981).
[10] M. J. Nadeau, M. A. Garwan, X. L. Zhao, and A. E. Litherland, Nucl. Instrum. Methods Phys. Res., Sect. B **123**, 521 (1997).
[11] V. T. Davis, J. T. Thompson, and A. Covington, Nucl. Instrum. Methods Phys. Res., Sect. B **241**, 118 (2005).
[12] Z. Felfli, A. Z. Msezane, and D. Sokolovski, Phys. Rev. A **78**, 030703 (2008).
[13] L. Pan and D. R. Beck, J. Phys. B: At., Mol. Opt. Phys. **43**, 025002 (2010).
[14] Z. H. Luo, X. L. Chen, J. M. Li, and C. G. Ning, Phys. Rev. A **93**, 020501 (2016).
[15] X. L. Chen, Z. H. Luo, J. M. Li, and C. G. Ning, Sci. Rep. **6**, 24996 (2016).
[16] X. L. Chen and C. G. Ning, Phys. Rev. A **93**, 052508 (2016).
[17] X. X. Fu, Z. H. Luo, X. L. Chen, J. M. Li, and C. G. Ning, J. Chem. Phys. **145**, 164307 (2016).
[18] A. T. J. B. Eppink and D. H. Parker, Rev. Sci. Instrum. **68**, 3477 (1997).
[19] A. Osterwalder, M. J. Nee, J. Zhou, and D. M. Neumark, J. Chem. Phys. **121**, 6317 (2004).
[20] I. Leon, Z. Yang, H. T. Liu, and L. S. Wang, Rev. Sci. Instrum. **85**, 083106 (2014).
[21] B. Dick, Phys. Chem. Chem. Phys. **16**, 570 (2014).
[22] C. S. Feigerle, Z. Herman, and W. C. Lineberger, J. Electron Spectrosc. Relat. Phenom. **23**, 441 (1981).
[23] X. B. Wang and L. S. Wang, Rev. Sci. Instrum. **79**, 073108 (2008).
[24] L. S. Wang, J. Chem. Phys. **143**, 040901 (2015).
[25] M. L. Weichman and D. M. Neumark, Annu. Rev. Phys. Chem. **69**, 101 (2018).
[26] D. M. Neumark, J. Phys. Chem. A **112**, 13287 (2008).
[27] E. P. Wigner, Phys. Rev. **73**, 1002 (1948).
[28] X. L. Chen and C. G. Ning, J. Phys. Chem. Lett. **8**, 2735 (2017).
[29] J. E. Sansonetti and W. C. Martin, J. Phys. Chem. Ref. Data **34**, 1559 (2005); or NIST Atomic Spectra Database version 5.0, 2012; http://www.nist.gov/pml/data/asd.cfm.